Cell

SIRT1 Suppresses β-Amyloid Production by Activating the α-Secretase Gene ADAM10

Gizem Donmez,[1] Diana Wang,[1] Dena E. Cohen,[1] and Leonard Guarente[1,*]
[1]Paul F. Glenn Laboratory and Department of Biology, Massachusetts Institute of Technology, Cambridge, MA 02139, USA
*Correspondence: leng@mit.edu
DOI 10.1016/j.cell.2010.06.020

SUMMARY

A hallmark of Alzheimer's disease (AD) is the accumulation of plaques of Aβ 1–40 and 1–42 peptides, which result from the sequential cleavage of APP by the β and γ-secretases. The production of Aβ peptides is avoided by alternate cleavage of APP by the α and γ-secretases. Here we show that production of β-amyloid and plaques in a mouse model of AD are reduced by overexpressing the NAD-dependent deacetylase SIRT1 in brain, and are increased by knocking out SIRT1 in brain. SIRT1 directly activates the transcription of the gene encoding the α-secretase, ADAM10. SIRT1 deacetylates and coactivates the retinoic acid receptor β, a known regulator of ADAM10 transcription. ADAM10 activation by SIRT1 also induces the Notch pathway, which is known to repair neuronal damage in the brain. Our findings indicate SIRT1 activation is a viable strategy to combat AD and perhaps other neurodegenerative diseases.

INTRODUCTION

Alzheimer's disease (AD) is a neurodegenerative disorder affecting up to one-third of individuals reaching the age of 80 (Tanzi and Bertram, 2005). It displays a stereotypical brain pathology; deposition of plaques of amyloid beta (Aβ) peptides and phosphorylation and tangles of the neurofibrillar protein τ (Hardy and Selkoe, 2002). Affected individuals suffer neurological damage resulting in memory loss, cognitive, and functional decline and death.

Insight into the etiology of AD has come from studies of the rare familial form of early onset AD (Selkoe, 1997). Dominant mutations have been found in the gene encoding the neuronal membrane protein amyloid precursor protein (APP), which can be cleaved in two sequential steps by the β- and γ-secretases to generate Aβ 1–40 and 1–42 amyloid peptides (Tanzi and Bertram, 2005). A second class of dominant mutations giving rise to familial AD fall in genes presenilin 1 and 2 (PSEN1 and 2), which encode components of the γ-secretase (De Strooper, 2007). These findings suggest a pathway of AD in which sequential cleavage of APP by the β and γ-secretases leads to accumulating β-amyloid and the downstream pathologies of AD, such as Aβ plaques, τ tangles, and neurodegeneration.

Interestingly, the production of Aβ peptides is avoided by an alternate APP cleavage pathway mediated by the α-secretase followed by the γ-secretase (Postina et al., 2004). Indeed, α-secretase cleavage of APP has been shown to be protective in AD models (Mattson, 1997; Kojro and Fahrenholz, 2005). The α- and γ-secretases also sequentially cleave the notch receptor to generate a notch intracellular domain (NICD) (Kojro and Fahrenholz, 2005; van Tetering et al., 2009). The NICD activates nuclear genes, such as HES1 and HES5 to facilitate neurogenesis during development and damage repair in adults (Kopan and Ilagan, 2009; Yoon and Gaiano, 2005; Costa et al., 2005). ADAM10 encodes the α-secretase (Saftig and Hartmann, 2005; Fahrenholz et al., 2008), and transcription of this gene is activated by the retinoic acid receptor (RAR) (Fahrenholz et al., 2008; Prinzen et al., 2005; Tippmann et al., 2009). Indeed, several studies suggest a link between retinoic acid (RA) signaling in the brain and AD (Goodman and Pardee, 2003; Corcoran et al., 2004; Goodman, 2006).

Sirtuins are NAD-dependent deacetylases that counter aging and have a wide spectrum of metabolic and stress-tolerance functions (Sinclair, 2005). Of the seven mammalian sirtuins, the SIR2 ortholog SIRT1 deacetylates numerous regulatory proteins, such as PGC-1α, p53, FOXO, HSF, and HIF-2α to trigger resistance to metabolic, oxidative, heat, and hypoxic stress (Guarente, 2009). SIRT1 has been directly implicated in neuronal protection against stress in cultured cells (Qin et al., 2006). In mice, SIRT1 has been shown to protect against neurodegeneration in the p25 overexpression model (Kim et al., 2007), as well as in Wallerian degeneration slow mice (Araki et al., 2004). More generally, SIRT1 mediates at least some of the effects of calorie restriction (Guarente, 2008), a diet reported to protect against models of neurodegenerative diseases, including AD (Patel et al., 2005).

Here, we investigate whether SIRT1 levels in brain affect the Aβ plaque formation, pathology, and cognitive decline in AD mouse model (APPswe/PSEN1dE9 double transgenic). We show that SIRT1 can suppress AD in a mouse model for this disease. The induction of brain pathology and behavioral deficits was mitigated in AD mice overexpressing SIRT1 in brain, and exacerbated with SIRT1 knocked out in the brain. SIRT1 directly activates transcription of ADAM10, which encodes the α-secretase by deacetylating RARβ. SIRT1 appears to direct APP processing toward the α-secretase and away from the β-secretase, which results in a reduction in the production of toxic β-amyloid

peptides. Furthermore, by activating ADAM10, which is also known to cleave the membrane-bound notch receptor thus liberating an intracellular domain that activates nuclear genes for neurogenesis, SIRT1 also activates notch pathway. As a result of this, SIRT1 helps to mitigate AD by increasing neurogenesis and neuroprotection that would be a second way besides suppressing β-amyloid production.

RESULTS

Effects of SIRT1 Levels in a Mouse Model of AD

We wished to test whether the levels of SIRT1 in the brain could influence Aβ plaque formation and the accruing pathological and cognitive decline in a mouse model of AD. We thus employed a model in which two linked transgenes, encoding the human APPswe and PSEN1dE9 alleles drive Aβ plaque formation and learning and memory deficits (Jankowsky et al., 2004). Plaques are evident in this model at 3–5 months of age, and they progress in number and size as mice grow older. In order to test the effects of increasing SIRT1 in these AD mice, they were crossed to strains bearing a SIRT1 transgenic allele (Tg in figures) that results in overexpression of the protein in the brain by about 2-fold (Bordone et al., 2007). Neither the SIRT1 transgene nor the knock-out allele described below affected expression of the APPswe or PSEN1dE9 disease genes (not shown). In all experiments, we compare congenic C57BL/6 littermates by quantifying cortical plaque number in serial coronal cross sections.

We observed a marked reduction of plaques in 5-month-old AD transgenic mice overexpressing SIRT1 (AD-Tg) compared to AD control mice (Figure 1A). Wild-type (WT) mice without the AD disease genes were free of plaques. In order to inactivate SIRT1 in the brain, we used brain-specific knock out mice (BSKO) (Cohen et al., 2009), which lack full length SIRT1 in all neurons and glia (Figure 1B), but show normal adult brain morphology (Figure S1A available online). To test the effects of SIRT1 inactivation, BSKO mice were crossed to AD mice. Remarkably, AD-BSKO mice all died between 3 and 5 months of age, whereas AD mice or BSKO mice themselves lived well past 1.5 years of age (Figure 1C and data not shown). Although we have not pinpointed the cause of death in AD-BSKO mice, this synthetic lethality is typically indicative of a strong genetic interaction between the genes involved, further linking SIRT1 to AD pathogenesis. Consistent with this, AD-BSKO mice displayed a marked increase in plaques in 3-month-old mice compared to AD control mice (Figure 1D).

In order to monitor other features of brain pathology, we assayed for gliosis by immunological quantitation of the glial marker of inflammation, glial fibrillary acidic protein (GFAP) (Panter et al., 1985). A progressive increase in cortical GFAP staining was observed in AD control mice, and this was markedly reduced in AD-Tg mice and exacerbated in AD-BSKO mice (Figure 1E). In addition, phosphorylation of τ at Ser199 and Ser399 (Johansson et al., 2006) was evident in AD mice and suppressed in AD-Tg mice (Figures S1B and S1C).

AD mice show age-dependent decline in learning and memory (Reiserer et al., 2007), which can be measured with behavioral tests. In the fear-conditioning test (Bryan et al., 2009), mice were trained on day 1 by repeated exposure to a tone followed by a foot shock (Figure 2A). Memory of this training is evinced on day 2 by a freezing behavior when exposed to the tone without the shock. AD control mice showed a progressive decline in performance in this test at 8 and 11 months of age compared to 4 and 6 months of age (Figure 2B). This decline was clearly suppressed in older, age-matched AD-Tg mice. Wild-type and SIRT1 transgenic mice without the AD genes showed roughly normal learning at all ages (Figure 2B). Conversely, AD-BSKO mice were precociously defective in this test at 4 months of age, whereas BSKO mice without the AD disease genes performed similar to wild-type mice (Figure 2C).

In the Morris water maze test, mice are trained to use visual cues to find a submerged platform in an opaque pool (Bryan et al., 2009). By determining the time required to find the platform (escape latency) as a function of days of training, we observed a marked decline in performance in 8- and 10-month-old AD mice compared to 4 month olds (Figure 2D). This decline was significantly mitigated in AD-Tg mice. In mice without the AD genes, the SIRT1 transgene had no effect at any ages (Figure 2E), indicating that the suppression of decline in AD-Tg mice is not due to an inherent increase in learning and memory in SIRT1 overexpressing mice. As in the fear conditioning test, AD-BSKO mice displayed a precocious defect at 4 months of age (Figure 2F). We observed no differences in swim speed in any mice tested (Figure S1D).

SIRT1 Activates α-Secretase and Reduces Production of β-Amyloid

Because Aβ plaques were reduced in SIRT1 transgenic mice, we quantitated Aβ levels in brains of AD mice overexpressing or lacking SIRT1 by ELISA. Strikingly, Aβ 1–42 levels were substantially reduced in AD-Tg mice and enhanced in AD-BSKO mice (Figure 3A). SIRT1 affected Aβ 1–40 in a like manner (Figure S2A). The reduction in Aβ levels in SIRT1 overexpressing mice was largest in 4-month-old mice and grew smaller, but was still evident, in older mice. A second assay using immunoblotting also showed similar effects on Aβ levels by SIRT1 (Figure S2B).

A reduction of Aβ levels by SIRT1 could reflect a reduced production of the amyloid peptides. To address the potential of mice to produce Aβ, we prepared brain extracts and assayed the α and β-secretases (Kojro and Fahrenholz, 2005; Fahrenholz et al., 2008; Rockenstein et al., 2005). Remarkably, AD-Tg mice showed a doubling of α-secretase activity in 2-, 4-, and 6-month-old mice compared to AD-controls (Figure 3B). Conversely, there was a small but significant reduction in BSKO mice with or without the AD genes.

In addition, we observed a small decrease in β-secretase activity (Figure 3C) and BACE1 (β-secretase) RNA (Figure S2C) in SIRT1 overexpressing mice at all ages. However, because β-secretase was induced by the progression of disease in AD mice (Fukumoto et al., 2004), it is likely that the small decrease in this activity in AD-Tg mice is a secondary consequence of a slower disease onset and progression. Consistent with this idea, β-secretase activity (Figure 3C) and BACE RNA levels (Figure S2C) were higher in AD-BSKO mice compared to AD mice. Examination of individual γ-secretase subunits pen2 (Figure S2D), Aph1a, Aph1b (Figure S2E), and presenilin 1 (Figure S2F) showed no differences in mice with altered levels of SIRT1.

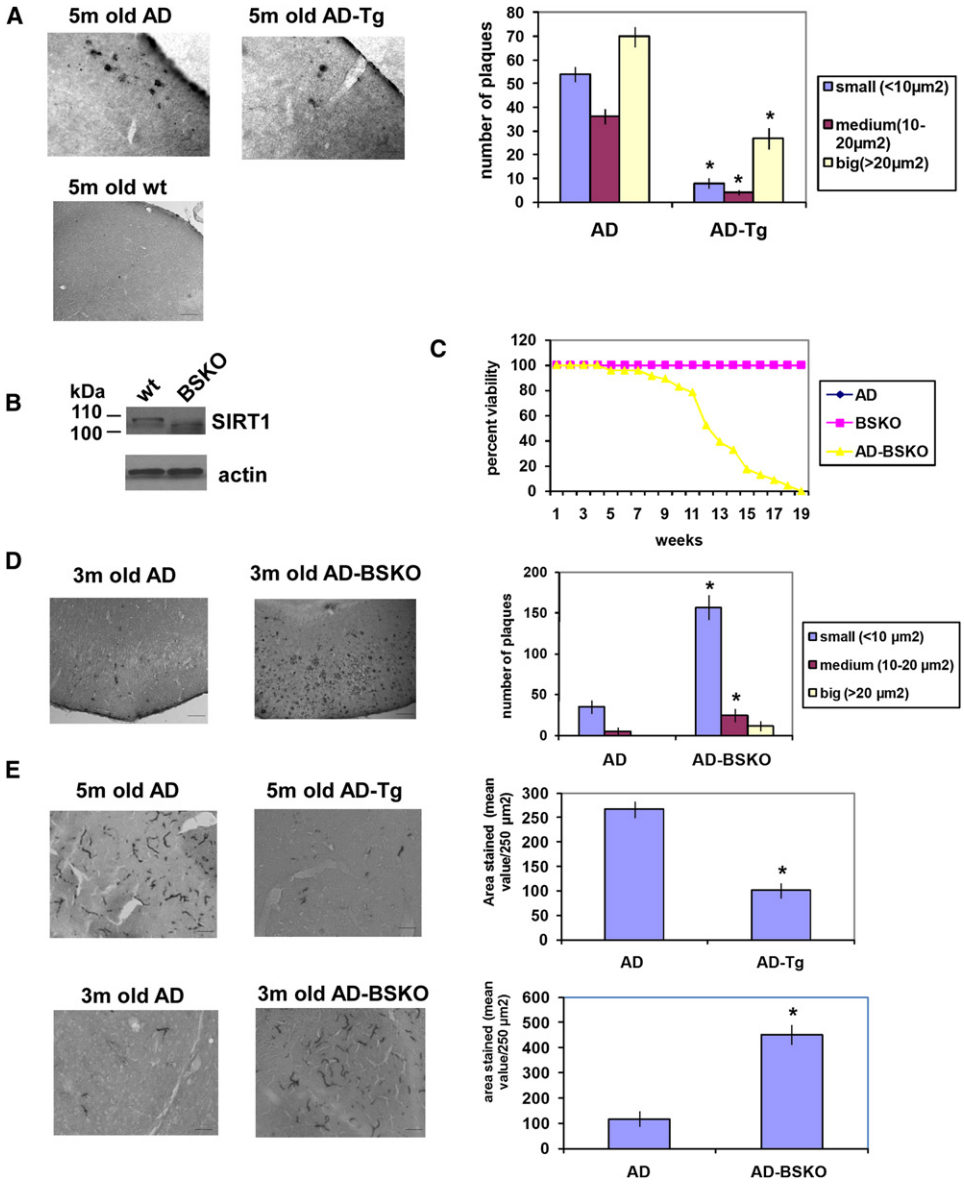

Figure 1. SIRT1 Levels Regulate the Pathology in a Mouse Alzheimer's Disease Model

(A) Cortical frozen sections (six per mouse) of fixed brains from indicated mice (ages in months [m]) stained with Aβ-specific 6E10 antibody. The graph on the right shows the quantification of the amyloid plaques according to their sizes in APPswe,PSEN1dE9 mice with endogenous SIRT1 (AD) and with a SIRT1 transgene (AD-Tg), n = 5. Left shows examples of stained samples from these and WT mice. Scale bar represents 50 μm. * indicates $p < 0.01$ throughout in Student's t test.

(B) Western blot analysis of SIRT1 expression in wild-type (wt) and SIRT1 brain specific knockout mouse (BSKO) whole brains. Deletion of exon 4 resulted in the truncated inactive form of SIRT1 in BSKO mice. β-actin served as a loading control.

(C) Survival curve of the percent viability of the AD, BSKO and AD-BSKO mice. n = 47 for AD-BSKO and BSKO and n = 45 for AD mice. Both BSKO and AD mice showed 100% viability.

(D) Cortical frozen sections of fixed brains from indicated mice stained with Aβ-specific 6E10 antibody. The graph on the right shows the quantification of the amyloid plaques. Scale bar represents 50 μm. n = 5.

(E) Frozen sections of fixed brains from indicated mice stained with GFAP (glial fibrillary acidic protein) antibody for gliosis. The graph on the right shows the quantification of the GFAP staining. Scale bar represents 50 μm.

The analysis was carried out using Student's t test. Significant differences are shown by single asterisk (*) indicating $p < 0.01$. Error bars represent SEM. See also Figure S1.

The above findings suggest that SIRT1 may suppress AD by directing APP processing toward the α-secretase. To obtain further evidence for this hypothesis, we quantitated two of the products of α-secretase cleavage. First, α-secretase generates a large α-fragment ectodomain of APP (Figure 3D), which migrates slightly faster than APP in a gel (Lesné et al., 2006; Vieira et al.,

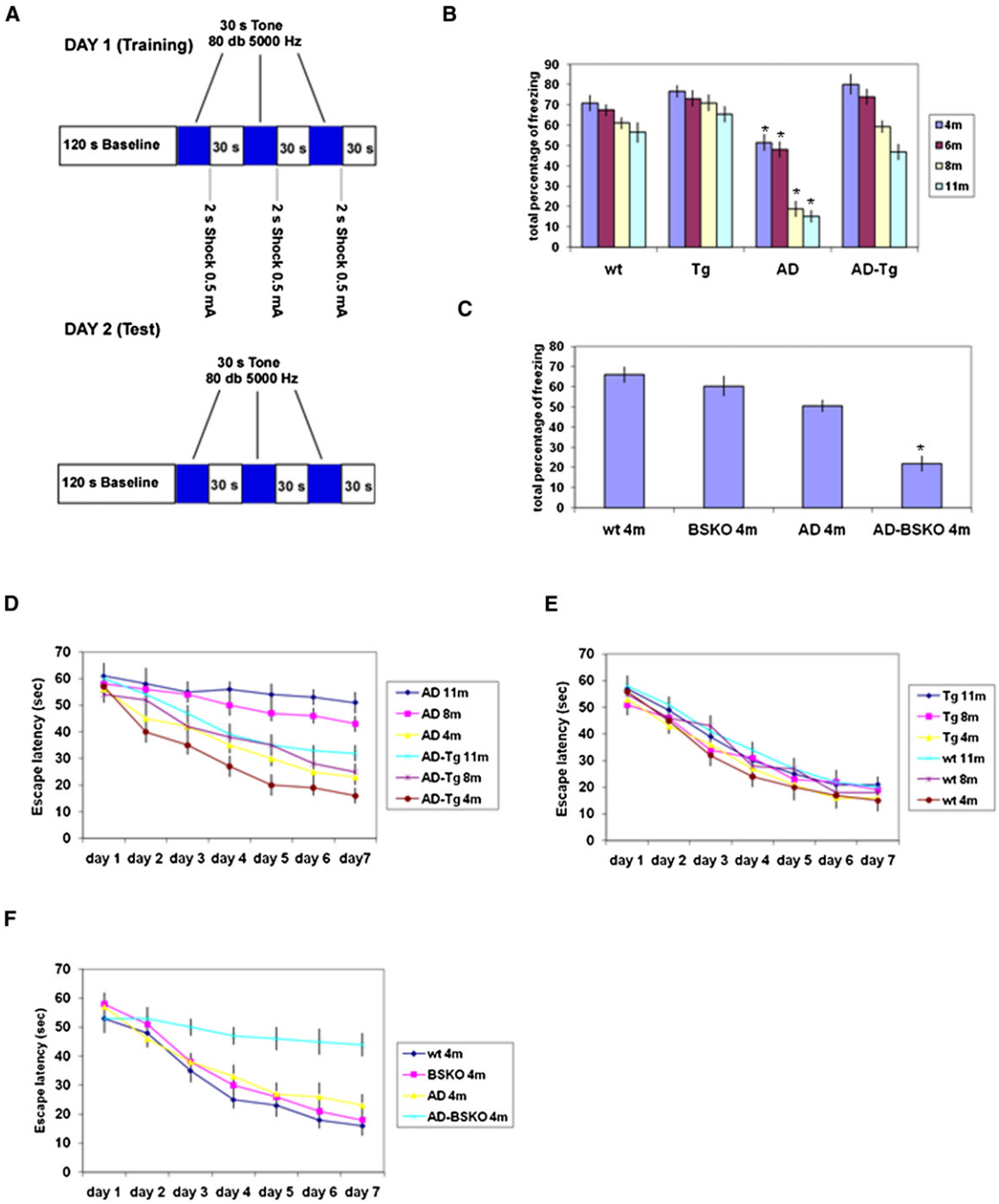

Figure 2. SIRT1 Improves the Behavioral Phenotype of Alzheimer's Disease Mouse Model

(A) Schema of the fear conditioning experiment.

(B) The graph shows the total percentage of freezing (on day 2) of the WT, Tg, AD, and AD-Tg mice of the indicated ages across the entire 5 min tone retrieval test. n = 10–15 for each bar.

(C) The graph shows the total percentage of freezing of the WT, BSKO, AD, and AD-BSKO mice at 4 months of age across the entire 5 min tone retrieval test. n = 10–15.

(D) Morris water maze experiment (D-F). Escape latency (time to find the platform) was plotted for 7 days for 11-, 8-, and 4-month-old AD and AD-Tg mice. n = 6–12.

(E) Escape latency plotted over 7 days for 11-, 8-, and 4-month-old Tg and WT mice. n = 6–12.

(F) Escape latency plotted over 7 days for 4-month-old WT, BSKO, AD and AD-BSKO mice. n = 6–12.

The analysis was carried out using Student's t test. Significant differences are shown by single asterisk (*) indicating $p < 0.01$. Error bars represent SEM. See also Figure S1.

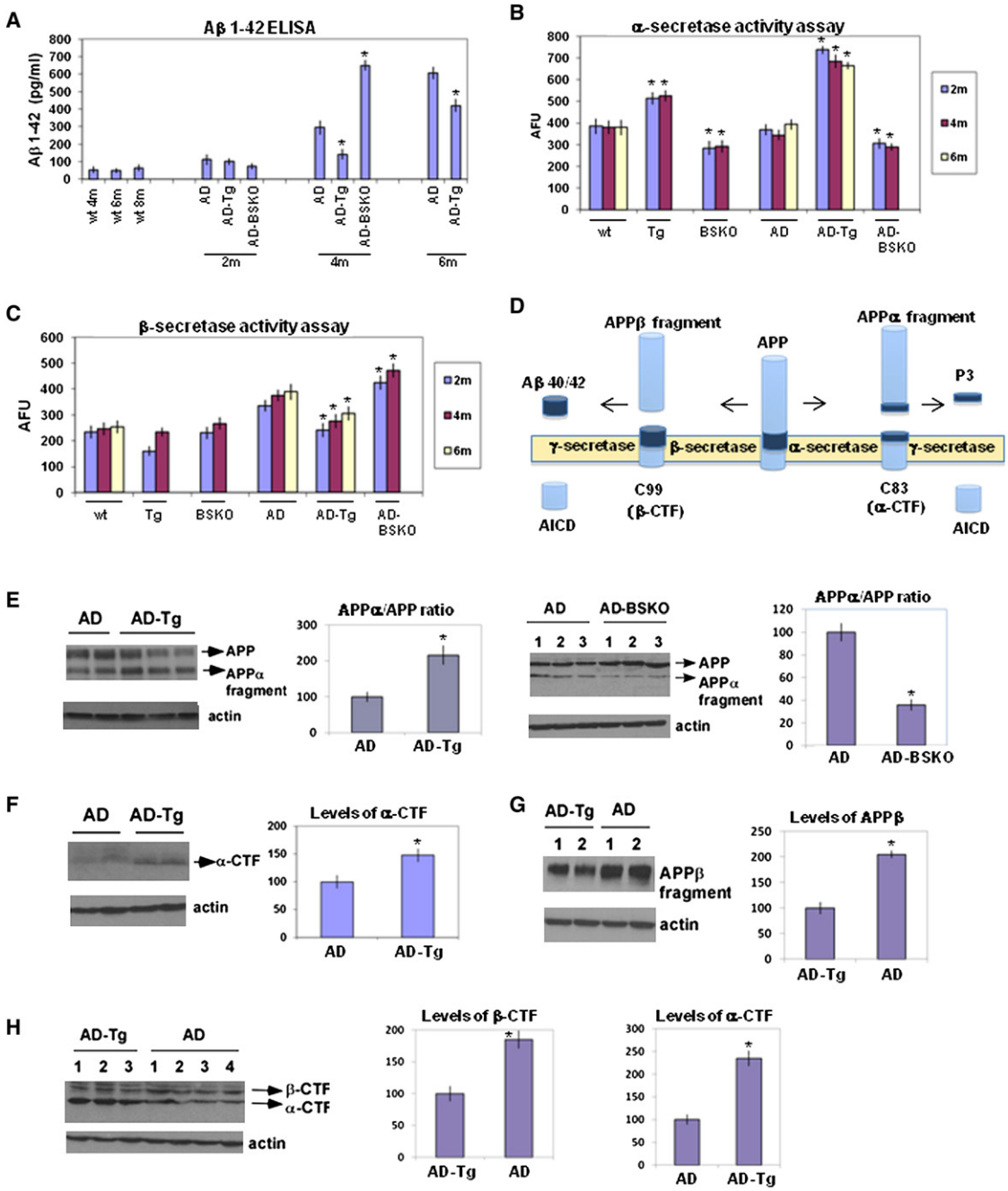

Figure 3. SIRT1 Reduces Aβ Levels and Increases α-Secretase Activity

(A) Aβ 1-42 levels measured using ELISA from the whole brains of the indicated mice. n = 6 for each bar.

(B) α-secretase activity from the whole brains of indicated mice using an activity assay. n = 6. AFU, arbitrary fluorescence units.

(C) β-secretase activity in the whole brains of indicated mice. n = 6.

(D) The scheme of the proteolytic processing of APP. Aβ 40/42, amyloid β peptide with 40 (Aβ 1-40), or 42 amino acid residues (Aβ 1-42); APP, amyloid precursor protein; AICD, APP intracellular domain; APPα, soluble APP after α-secretase cleavage (α-fragment); APPβ, soluble APP after β-secretase cleavage; C99, C-terminal fragment of APP of 99 amino acids after β-secretase cleavage; C83, C-terminal fragment of APP of 83 amino acids after α-secretase cleavage (α-CTF); P3, N-terminal fragment of C83 after α-secretase cleavage.

(E) Western blotting of the whole brains of indicated mice of 6 months of age using 6E10 antibody. β-actin serves as the loading control. Quantification of the APPα/APP ratio is shown on the right as percent of control.

(F) Western blotting of the whole brains of indicated mice of 6 months of age using APP C-terminal antibody. β-actin serves as the loading control. Quantification of the α-CTF is shown on the right as percent of control.

2009). The ratio of α-fragment to APP was clearly increased in AD-Tg mice and decreased in AD-BSKO mice (Figure 3E). We have also determined the levels of α-fragment by using an α-fragment-specific antibody (APPα antibody), and observed that the levels of α-fragment in AD-Tg mice is increased compared to AD mice (Figure S2G). Second, the other product of APP cleavage by α-secretase is a fragment termed α-CTF (Lesné et al., 2006; Vieira et al., 2009) (Figure 3D), and again, levels of this protein were increased in AD-Tg mice (Figures 3F and 3H, performed by using two different antibodies). We have also analyzed the products of APP cleavage by β-secretase (Figure 3D), β-fragment, and β-CTF. Both were decreased in AD-Tg mice compared to AD mice (Figures 3G and 3H). Together, all of the above findings indicate that α-secretase is activated by SIRT1.

SIRT1 Activates ADAM10 Transcription and Notch Pathway

We next determined RNA levels in the brain of ADAM10, which encodes the α-secretase (Saftig and Hartmann, 2005; Fahrenholz et al., 2008) and found a significant increase in SIRT1 overexpressing mice with or without the AD disease genes (Figure 4A). Conversely, AD-BSKO mice showed a significant decrease in ADAM10 RNA. We also observed elevated levels of ADAM10 and its precursor ADAM10-P in SIRT1 overexpressing mice with (Figure 4B, left panel; Figure S3A) or without (Figure 4B, middle panel) the AD genes, and decreased levels in AD-BSKO mice (Figure 4B, right panel). The ADAM10 homologs ADAM 9 and ADAM 17 (Saftig and Hartmann, 2005) did not show clear changes in SIRT1 overexpressing or BSKO mice with or without the AD disease genes (Figure S3B).

What might be the biological relevance of SIRT1 activation of ADAM10? This protease is known to cleave the notch receptor to release a *n*otch *i*ntra*c*ellular *d*omain (NICD), which activates transcription of genes involved in neurogenesis and patterning during embryonic development and the maintenance of brain function in adults (Yoon and Gaiano, 2005; Costa et al., 2005). To determine whether SIRT1 regulates the notch pathway in adults, we first quantitated levels of the NICD in brain extracts. SIRT1 Tg mice with or without the AD disease genes showed a significant elevation in NICD levels in AD-Tg mice compared to AD controls (Figure 4C). Moreover, transcription of the notch nuclear target genes HES1 and HES5 (Kopan and Ilagan, 2009; Yoon and Gaiano, 2005) were also significantly elevated in AD-Tg mice compared to AD mice (Figure 4D).

Activation of ADAM10 Depends on Deacetylase Activity of SIRT1 and Retinoic Acid

The above findings suggest that SIRT1 is a positive activator of ADAM10 transcription. Consistent with this surmise, chromatin immunoprecipitation assays revealed direct interaction of SIRT1 with a specific region of the ADAM10 promoter −467 to −30 but not −2100 to −1900 (Figure 5A; Figure S4A). This gene-proximal region of ADAM10 is where the RAR is known to bind and activate transcription (Prinzen et al., 2005). Cellular effects of RA are mediated by the RARs and retinoic X receptors (RXRs), which form heterodimers and bind to retinoic acid response element (RAREs) to activate gene expression (Mangelsdorf and Evans, 1995).

We next investigated the mechanism of ADAM10 activation by SIRT1 in cultured cells. SIRT1 or the catalytically inactive and dominant negative mutant His363-Tyr (SIRT1HY) were expressed in mouse embryo fibroblasts (MEFs) from SIRT1$^{+/+}$ and SIRT1$^{-/-}$ embryos (Figure S4B) and endogenous ADAM10 RNA (Figure 5B) or NICD levels (Figure 5C) were quantitated. Expression of SIRT1 but not SIRT1HY increased levels of ADAM10 RNA and NICD protein in SIRT1$^{-/-}$ MEFs, indicating that the deacetylase activity of SIRT1 is required for ADAM10 activation. Further, addition of RA also increased ADAM10 RNA and NICD protein in SIRT1$^{+/+}$ but not SIRT1$^{-/-}$ MEFs, and this activation was further enhanced by SIRT1 and blocked by SIRT1-HY. These findings suggest that the RAR is the target of SIRT1 activation of ADAM10. To bolster this claim, we also expressed SIRT1 or SIRT1-HY in N2A neuroblastoma cells (Figure S4C). Expression of SIRT1 but not SIRT1-HY activated ADAM10 RNA (Figure S4D) and NICD protein levels (Figure S4E) in N2A cells. Further, addition of RA also increased ADAM10 RNA and NICD protein, and this activation was further enhanced by SIRT1 and blocked by SIRT1-HY as in MEF cells.

SIRT1 Deacetylates Retinoic Acid Receptor β

SIRT1 is known to deacetylate numerous mammalian transcription factors (Donmez and Guarente, 2010). To further investigate the relationship between SIRT1 and the RAR, we studied a luciferase reporter driven by the RARE in MEFs (Figure 6A). Luciferase levels were activated by SIRT1 overexpression and reduced in SIRT1$^{-/-}$ MEFs. Moreover, addition of RA-stimulated luciferase while preserving the differences in SIRT1 overexpressing and SIRT1$^{-/-}$ MEFs. In contrast, the RAR antagonist LE 135 (Li et al., 1999) blocked activity in all cases. These findings clearly indicate that SIRT1 coactivates the RAR. Next, we carried out immunoprecipitation of endogenous SIRT1 on antibody-coated beads (Figure 6B). We observed coimmunoprecipitation of endogenous RARβ, the major isoform in the brain (Mangelsdorf and Evans, 1992; Dollé et al., 1990). As a specificity control, we checked LXR levels (another nuclear receptor) in the immunoprecipitates and observed none (Figure S5A). Finally, we found that acetylation of endogenous RARβ was enhanced in SIRT1$^{-/-}$ cells and reduced in SIRT1 overexpressing cells, further indicating that SIRT1 coactivates RARβ by deacetylating it (Figure 6C). Also, acetylation of endogenous RARβ was

(G) Western blotting of the whole brains of indicated mice of 6 months of age using APPβ antibody. β-actin serves as the loading control. Quantification of the APPβ fragment is shown on the right as percent of control.

(H) Western blotting of the whole brains of indicated mice of 6 months of age using a different APP C-terminal antibody (see Experimental Procedures) from Figure 3F that can detect both α-CTF and β-CTF. β-actin serves as the loading control. Quantification of the α-CTF and β-CTF are shown on the right as percent of control.

The analysis was carried out using Student's t test. Significant differences are shown by single asterisk (*) indicating $p < 0.01$. Error bars represent SEM. See also Figure S2.

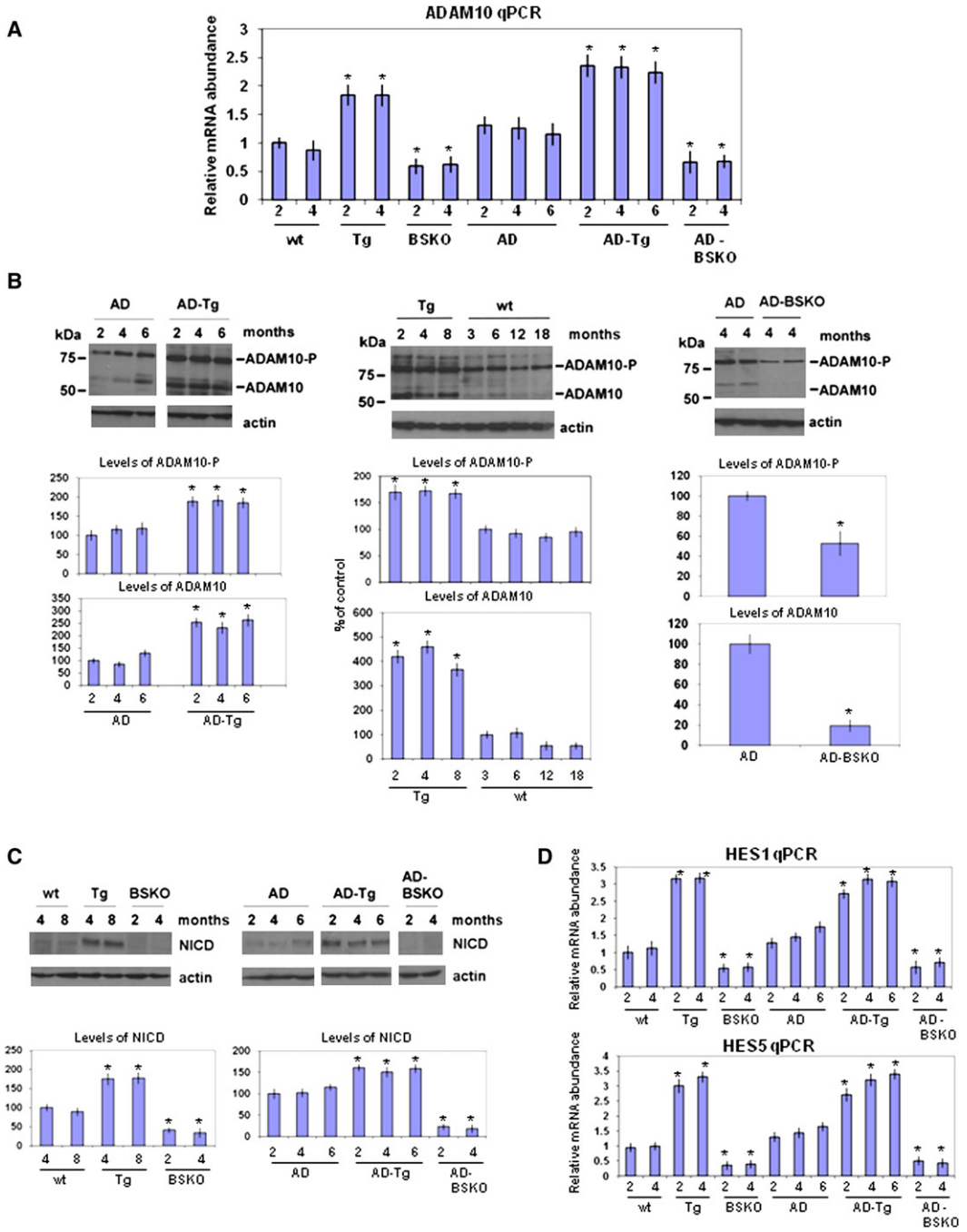

Figure 4. SIRT1 Increases α-Secretase Levels by Activating ADAM10

(A) ADAM10 RNA levels from whole brains of indicated mice quantified by q-PCR. The numbers on x axis show the age of mice in months. n = 5 for each bar.

(B) Western blotting of whole brains from mice of indicated ages in months (m) and years (y) using ADAM10 antibody. β-actin serves as the loading control. ADAM10-P shows the unprocessed ADAM10 precursor protein. Quantification of ADAM10-P (top) and ADAM10 (bottom) are shown below each gel as percent of control.

(C) Western blotting of whole brains from indicated mice using NICD (Notch intracellular domain) antibody. β-actin serves as the loading control. Quantification of NICD is shown below as percent of control.

(D) HES1 and HES5 RNA levels quantified from whole brains of mice by q-PCR. The numbers on x axis show the age of mice in months. n = 5.

The analysis was carried out using Student's t test. Significant differences are shown by single asterisk (*) indicating $p < 0.01$. Error bars represent SEM. See also Figure S3.

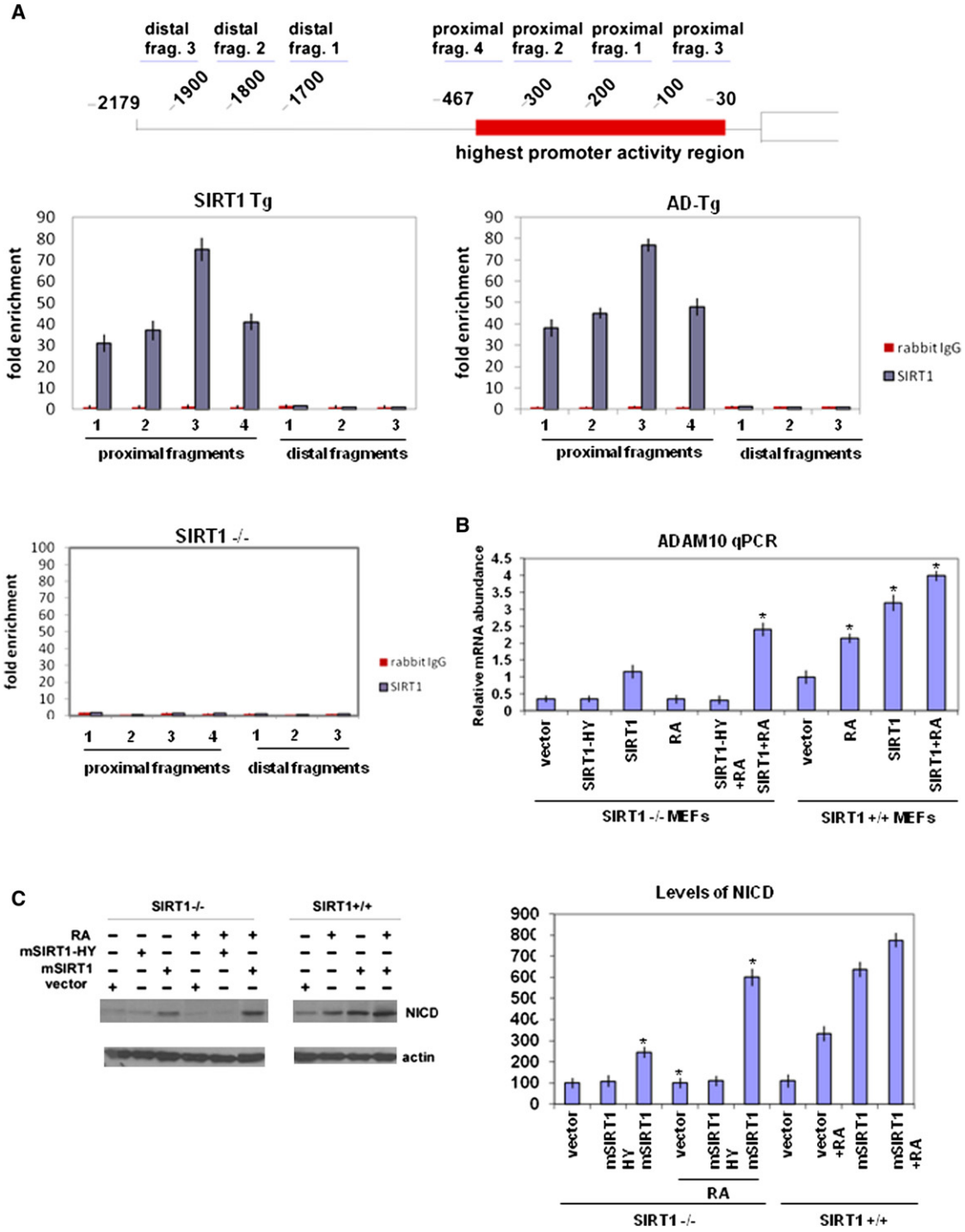

Figure 5. SIRT1 and RA directly activate ADAM10

(A) Chromatin-immunoprecipitation on whole brains of 6-month-old SIRT1 Tg, AD-Tg, and SIRT1$^{-/-}$ mice with anti-SIRT1 antibody or IgG. The scheme illustrates the highest activity region of the ADAM10 promoter and the fragments generated by primers in qPCR assay. q-PCR was performed using primers as indicated (see Experimental Procedures). SIRT1$^{-/-}$ mice were in a mixed genetic background to allow recovery of viable adults (McBurney et al., 2003).

(B) ADAM10 RNA levels quantified by q-PCR from the SIRT1$^{+/+}$ or SIRT1$^{-/-}$ MEFs transfected with mSIRT1 or mSIRT1-HY and/or treated with retinoic acid (RA).

(C) NICD levels determined by western blotting from the SIRT1$^{+/+}$ or SIRT1$^{-/-}$ MEFs transfected with mSIRT1 or mSIRT1-HY and/or treated with retinoic acid (RA). β-actin serves as the loading control. Quantification of NICD levels is shown on the right as percent of control.

The analysis was carried out using Student's t test. Significant differences are shown by single asterisk (*) indicating $p < 0.01$. Error bars represent SEM. See also Figure S4.

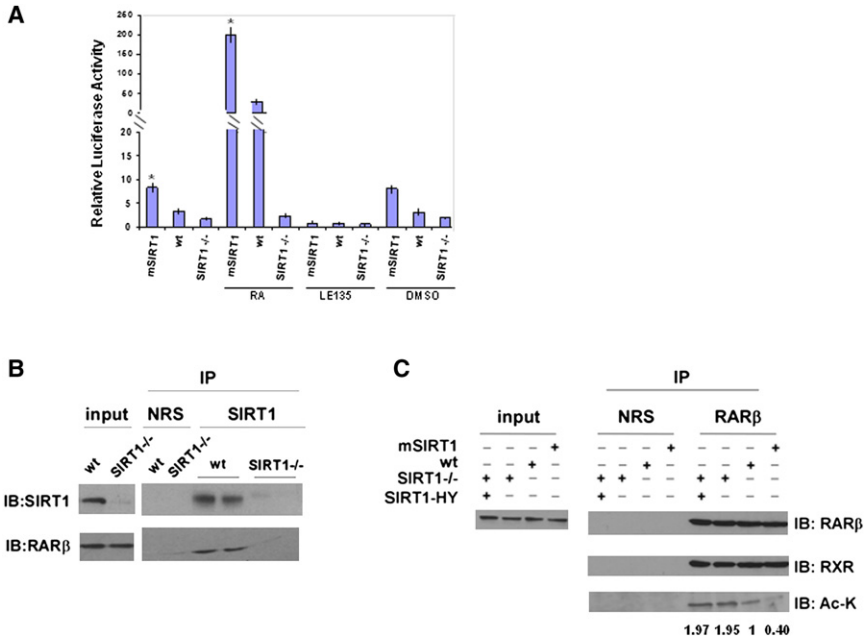

Figure 6. SIRT1 Deacetylates RARβ

(A) Luciferase reporter assays of MEFs overexpressing SIRT1 (mSIRT1), lacking SIRT1 ($SIRT1^{-/-}$), or controls (wt). Cells were transfected with luciferase reporter driven by the RARE (Retinoic Acid Receptor Element). Twenty-four hours later, cells were incubated with RA (Retinoic Acid), LE-135, or DMSO for an additional 24 hr and assayed as described in Experimental Procedures.

(B) Cell lysates from wild-type (wt) and $SIRT1^{-/-}$ ($SIRT1^{-/-}$) MEFs immunoprecipitated with normal rabbit serum (NRS) or anti-SIRT1 antibody and blotted with anti-SIRT1 and anti-RARβ antibodies. The two proteins are shown to interact at endogenous levels.

(C) Cell lysates from wild-type (wt), SIRT1-overxpressing (mSIRT1) MEFs, $SIRT1^{-/-}$ MEFs, and $SIRT1^{-/-}$ MEFs overexpressing SIRT1 catalytic mutant HY were subjected to immunoprecipitation with anti-RARβ antibody or NRS. Immunoprecipitates were analyzed by western blotting with anti-RARβ, anti-RXR, or anti-pan acetylated lysine (Ac-K) antibodies. Quantification of the acetylation levels were shown below (see also Figure S5).

(D) A model for the role of SIRT1 in suppressing Aβ production and activating notch pathway. SIRT1 deacetylates RARβ, causes RA to bind to RARβ-RXR heterodimer that binds to ADAM10 promoter. ADAM10 transcription and protein level is increased and APP processing is directed toward α-secretase pathway. This will lead to less β-secretase cleavage of APP resulting in less Aβ production, fewer β-amyloid plaques, and less gliosis. ADAM10 activation by SIRT1 also induces the Notch pathway, which is known to repair neuronal damage in brain, providing neuroprotection. The analysis was carried out using Student's t test. Significant differences are shown by single asterisk (*) indicating $p < 0.01$. Error bars represent SEM. See also Figure S5.

unaffected by expressing catalytic mutant of SIRT1, SIRT1-HY in $SIRT1^{-/-}$ cells, indicating that catalytic domain of SIRT1 is required for deacetylation. We did not observe acetylation of endogenous RARα when identical immunoprecipitation experiments were performed using RARα antibody (Figure S5B), indicating the effects of SIRT1 are specific for RARβ.

SIRT1 Suppresses Aβ Production Because It Activates ADAM10

Does the increase in ADAM10 in SIRT1 overexpressing mice account for the reduction in β-amyloid production? To address this question, we assayed Aβ1–42 produced by N2A neuroblastoma cells expressing the APPswe and PSEN1dE9 transgenes (Borchelt et al., 1996). Overexpression of SIRT1 in these cells substantially increased ADAM10 (Figure 7B) and reduced Aβ levels (Figure 7A) compared to control cells, analogous to what we observed in mice. Conversely, silencing ADAM10 with three different shRNAs alone (Figure 7B) increased Aβ (Figure 7A). Of critical importance, in cells overexpressing SIRT1, ADAM10-shRNAs reduced ADAM10 to levels of control cells (Figure 7B) and also prevented the suppression in Aβ production by this sirtuin (Figure 7A). We also employed scrambled shRNA as control that did not have any silencing effect on ADAM10 (Figures S6A–S6C). This finding indicates SIRT1 overexpression reduces Aβ production by increasing ADAM10. Finally, as in the mice, the reduction of SIRT1 levels (by three different shRNAs 1, 2, and 3) increased Aβ production in these cells (Figures 7A and 7B; Figure S6D). As a test for the specificity of these ADAM10 shRNAs, we showed that their effects were rescued by expressing ADAM10 mutant genes that were resistant to shRNA 1 or an siRNA to the ADAM10 3′ UTR (Figures S6E and S7A).

Correspondingly, NICD levels (Figure 7C) and expression of the notch targets HES1 (Figure 7D) and HES5 (Figure S7B) were increased by SIRT1 overexpression and decreased by shRNA for SIRT1 or ADAM10 in these cells. Most importantly, shRNA for ADAM10 reversed the increase in notch activity in SIRT1 overexpressing cells (Figures 7C and 7D). The above analysis draws a causal link between SIRT1 expression, ADAM10 activation, and Aβ suppression. A recent report showed that SIRT1 could affect α-secretase activity in cultured cells by inhibiting expression of the rho-associated protein kinase ROCK1 (Qin et al., 2006). However, we observed no differences in ROCK1 levels in mice with altered levels of SIRT1 (Figure S7C).

In order to show that RARβ activation by SIRT1 suppresses Aβ production, we treated N2A neuroblastoma cells expressing the APPswe and PSEN1dE9 transgenes with RA and RAR antagonist LE135. RA decreased Aβ production thereby augmenting the SIRT1 effect, whereas LE135 increased Aβ production thereby blocking the effect of SIRT1 (Figure 7E). These data show that RARβ activation by SIRT1 affects Aβ production.

DISCUSSION

Our findings clearly indicate that SIRT1 can suppress AD in a mouse model for this disease. The induction of brain pathology and behavioral deficits in doubly transgenic APPswe/PSEN1dE9 mice was mitigated in mice overexpressing SIRT1 in the brain, and exacerbated in mice with SIRT1 knocked out in the brain.

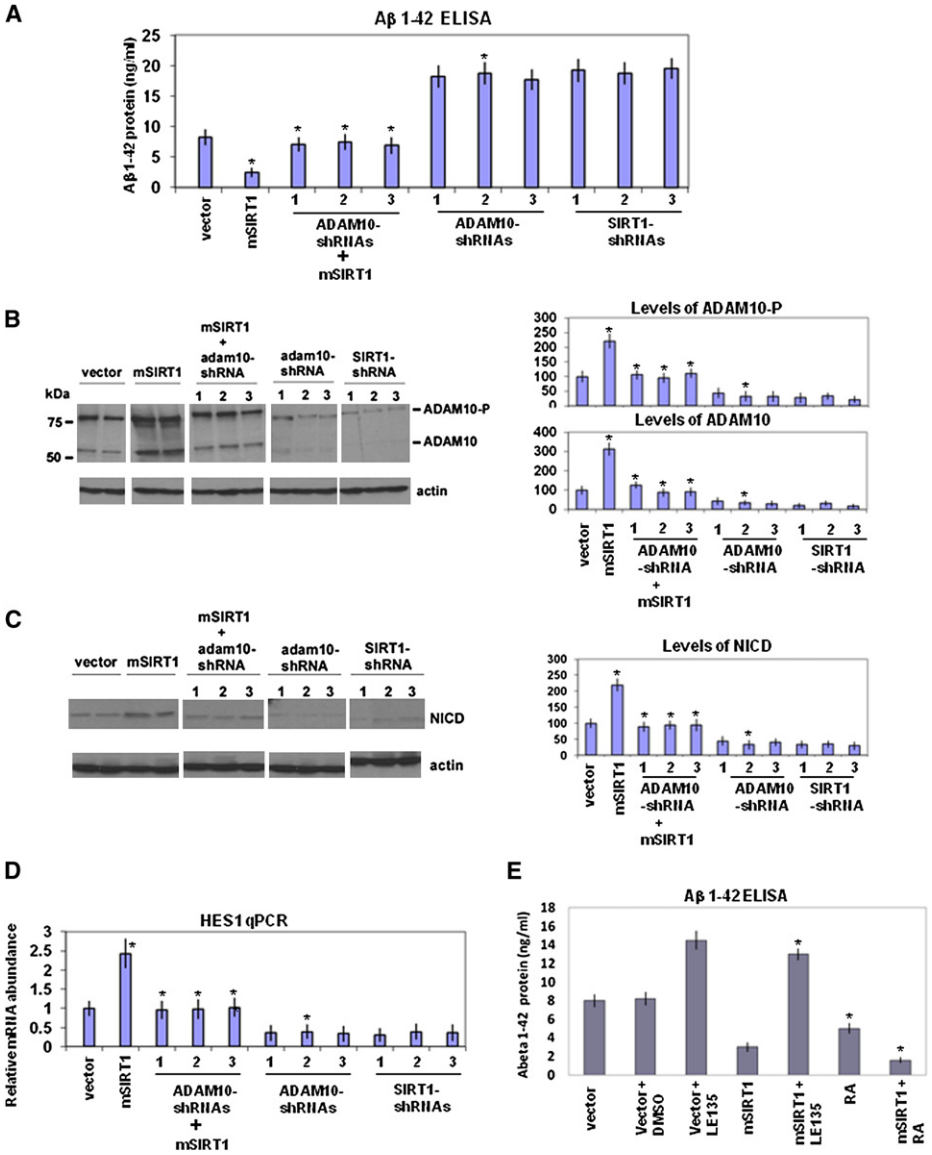

Figure 7. SIRT1 Suppresses Aβ Production by Activating ADAM10

(A) N2A cells stably overexpressing APPswe/PSEN1dE9 transgenes transfected with SIRT1 (mSIRT1). Twenty-four hours after SIRT1 transfection, cells were transfected with three different ADAM10-shRNA vectors (1, 2, or 3). N2A cells not overexpressing SIRT1 were also transfected with three different ADAM10-shRNA vectors (1, 2, or 3) to silence ADAM10. Separately, SIRT1 was silenced by three different shRNAs (1, 2, or 3). Forty-eight hours later, Aβ 1–42 concentration in the conditioned medium was assessed by ELISA (Experimental Procedures). N2A cells without APPswe,PSEN1dE9 transgenes showed no detectable Aβ 1–42 in this assay (not shown).

(B) Western blotting of the extracts of these cells using anti-ADAM10 antibody. Quantification of the ADAM10-P (top) and ADAM10 (bottom) were shown on the right as percent of control.

(C) Western blotting of the extracts of the cells using anti-NICD antibody. Quantification of the NICD are shown on the right as percent of control.

(D) HES1 RNA levels were determined by qPCR from RNA extracted from cells.

(E) N2A cells stably overexpressing APPswe/PSEN1dE9 were transfected with SIRT1 (mSIRT1). Twenty-four hours later, cells were incubated with RA (Retinoic Acid), LE-135, or DMSO for an additional 24 hr and assayed by ELISA.

The analysis was carried out using Student's t test. Significant differences are shown by single asterisk (*) indicating $p < 0.01$. Error bars represent SEM. See also Figures S6 and S7.

SIRT1 appears to direct APP processing toward the α-secretase and away from the β-secretase, which results in a reduction in the production of toxic β-amyloid peptides (Figure 6D). Indeed, SIRT1 directly activates transcription of ADAM10, which encodes the α-secretase. ADAM10 is also known to initiate activation of the notch pathway by cleaving the membrane-bound notch receptor thus liberating an intracellular domain that activates nuclear genes for neurogenesis (Costa et al., 2005;

Hartmann et al., 2001). Studies in neuroblastoma cells show that the suppression of Aβ production by SIRT1 is prevented by normalizing ADAM10 levels with specific shRNAs. Thus we conclude that the activation of ADAM10 by SIRT1 is mechanistically linked to Aβ suppression.

The mechanism of activation of ADAM10 by SIRT1 appears to be deacetylation of the RARβ, which is known to activate ADAM10 transcription. SIRT1 but not a catalytically inactive mutant activated ADAM10 transcription and the notch pathway in neuroblastoma cells and MEFs. Moreover, SIRT1 coactivated RAR in reporter assays, bound to the receptor at endogenous levels, and determined its acetylation level. SIRT1 has also been shown to deacetylate and regulate other members of the nuclear receptor family, such as LXR, PPARγ, PPARα, and the androgen receptor.

We can not be certain that the reduction in Aβ production in SIRT1 overexpressing mice is the sole mechanism conferring protection against memory decline in AD mice. First, activation of notch or perhaps other pathways by the increase in ADAM10 may also contribute to AD protection, because this pathway mediates repair in response to neuronal damage in the brain (Vieira et al., 2009; Mangelsdorf and Evans, 1995). Second, SIRT1 may also increase stress tolerance in neurons of the AD brain. Third, RAR targets other than ADAM10 may play some role in protection because RAR signaling is known to be disrupted in the AD brain (Goodman and Pardee, 2003; Corcoran et al., 2004; Goodman, 2006). However, we can be confident that the increase in ADAM10 and resulting reduction in Aβ will benefit AD mice. Indeed, ADAM10 has been shown to prevent amyloid plaque formation and hippocampal behavioral defects in AD mice (Postina et al., 2004). Further, ADAM10 mutations have been associated with a reduction in α-secretase in familial late-onset AD (Kim et al., 2009).

Mutations that severely reduce notch signaling result in embryonic lethality, because of a deficit in brain development (Yoon and Gaiano, 2005). Brain-specific SIRT1 KO mice activate cre in early embryos, yet are born in expected numbers and do not display any detectable defects in adult brain morphology or in performing behavioral tasks. It is possible that the reduction of notch signaling in the absence of SIRT1 is not sufficiently severe to cause dysfunction during embryonic development. Alternatively, the activation of notch by SIRT1 may have evolved for maintenance of the adult brain, rather than development.

SIRT1 has been implicated in protection against metabolic syndrome and diabetes, and sirtuin activators may offer promising new treatments for these increasingly common disorders (Milne et al., 2007). Recent studies also implicate SIRT1 in tumor protection, at least in some mouse models (Firestein et al., 2008). Our findings indicate that another important disease of aging, Alzheimer's Disease, is also mitigated by genetic activation of SIRT1. It may therefore be critically important to develop sirtuin activators tailored to cross the blood brain barrier to treat neurodegenerative diseases. The broad efficacy of SIRT1 activation in treating diseases of aging may derive from evolutionary selection for tissue maintenance to allow for delayed reproduction in the face of dietary or other stressors. The challenge is to harness this protection pharmacologically in a developed world, in which many of these stressors no longer exist.

EXPERIMENTAL PROCEDURES

Mouse Strains

All mice used were in congenic C57Bl/6 except SIRT1$^{-/-}$ mice for CHIP assay. Double transgenic (APPswe,PSENdE9) AD mouse model was purchased from Jackson Laboratory. SIRT1 transgenic mice have been described previously (Bordone et al., 2007). SIRT1 brain-specific knockout mice were generated by crossing a SIRT1 allele containing a floxed exon 4 (Cheng et al., 2003) with Cre-expressing mice driven by the brain-specific nestin promoter (Cohen et al., 2009). All mice were housed at controlled temperature (25°C) and 12:12 hr light/dark cycle.

Immunohistochemistry

Mice were perfused with 4% paraformaldehyde, cryoprotected, sectioned 40 μm-thick, and collected at 150-μm intervals. Six sections per brain were analyzed and consecutive sections of cortex were used for Aβ and GFAP staining. Vectastain kit (Vector Laboratories) were used to perform Aβ and GFAP staining according to manufacturer's directions. Thionin staining was performed as described (Pozniak et al., 2002). For Aβ and GFAP stainings, 6E10 (Covance) and GFAP (Abcam) antibodies were used, respectively. The plaque numbers, the sizes of the plaques, and GFAP staining were quantified using NIH ImageJ program.

Western Blotting and Immunoprecipitation

Mouse brains were homogenized in RIPA buffer (50 mM Tris-HCl pH: 8.0, 1 mM EDTA, 0.1% SDS, 150 mM NaCl, 1% NP40, 0.1% sodium-deoxycholate) including Complete Protease Inhibitor mixture (Roche), centrifuged, 100 μg of the supernatant was loaded onto 4%–15% gradient SDS-PAGE gels and immunoblotted with anti-SIRT1 (Upstate), 6E10, APPα, APPβ, APP C-terminal (Covance, Figure 3F), APP C-terminal (Santa Cruz, Figure 3H), ADAM10, ADAM10-Prodomain, ADAM9, ADAM17, Aph1a, Aph1b, Pen2, Rock1, NICD, p-τ Ser399, RARα, RARβ, RXR, LXR (Abcam), Presenilin1 (Cell Signaling), and Ac-K (Immuno-chem) antibodies. In order to separate the APPα fragment from APP (Figure 3E), 10%–20% SDS-PAGE gels were used and run for 2.5 hr. For western blotting using cells, cells were harvested and extracted in RIPA buffer as explained above. Proteosome inhibitors were used when analyzing NICD. Western blotting experiments were performed with at least three mice from each genotype and age and representative data are shown.

The immunoprecipitations were carried out by using Pierce Direct IP Kit (Thermo Scientific). Immobilizing the antibody covalently to agarose beads, this method results in purified antigen free from antibody contamination To show the endogenous interaction between SIRT1 and RARβ, anti-SIRT1 antibody or normal rabbit serum (NRS) was coupled to beads, and then WT and SIRT1$^{-/-}$ (SIRT1$^{-/-}$) MEFs were incubated with the beads. To determine RARβ acetylation, anti-RARβ antibody or NRS was coupled to beads, and then WT, SIRT1$^{-/-}$ (SIRT1$^{-/-}$), SIRT1$^{-/-}$ overexpressing SIRT1-HY, and SIRT1-overexpressing (mSIRT1) MEFs were incubated with the beads. The eluate was blotted with anti-SIRT1, anti-RARβ, and anti-Ac-K antibodies.

Fear Conditioning

10-15 mice from each indicated genotype and age were trained and tested in a fear conditioning device containing one observation chamber (30 × 24 × 21 cm; MED-Associates, Inc.). Fear to the tone was assessed by measuring freezing behavior. The output from video camera mounted in the chamber was fed into a video processor, and the mice were videotaped throughout each of the sessions. Freezing behavior, defined as the absence of all movements except for the breathing, was scored by the computer program. Freezing was quantified by computing the percentage of observations in which the mouse had been scored as freezing during test. The experimenter was blind to the genotypes and ages of the mice.

Morris Water Maze

Morris water maze testing procedure has been described previously (Bryan et al., 2009; Cao et al., 2007). Six to 12 mice from each indicated genotype and age were trained to find the visible platform three trials a day for the first day and tested to find the hidden platform for 7 consecutive days. In each trial, the mice were allowed to swim until it found the hidden platform, or until 2 min

had elapsed and, at which point the mouse was guided to the platform. The mouse was then allowed to sit on the platform for 10 s before being picked up. During the test days, the platform was hidden 1 cm beneath the water. The escape latency was recorded by a video camera. The experimenter was blind to the genotypes and ages of the mice. The swim speed of each mouse was calculated by video tracking system and MATLAB software.

ELISA and Secretase Activity Assays

Aβ 1–42 and Aβ 1–40 levels of brain tissue were quantitated by using Aβ 1–42 and Aβ 1–40 ELISA kits (Biosource), respectively. Phosphorylation levels of p-τ Ser199 was quantitated by using ELISA (Sigma). α- and β-secretase activities were quantitated by using α- and β-secretase activity assay kits (R&D Systems), respectively. Aβ 1–42 levels of the conditioned media from APPswe/PSEN1dE9 cells were measured by using Aβ 1–42 ELISA kit (Biosource). All ELISA and secretase activity assays were performed according to the manufacturer's directions.

RNA Isolation and Analysis

Total RNA from mouse brains was isolated by using Trizol (QIAGEN). For real time q-PCR analysis, cDNA was synthesized from total RNA by SuperScript III reverse transcriptase (Invitrogen) with random primers. The cDNA was then subjected to PCR analysis with gene specific primers in the presence of CYBR green (Bio-Rad). Relative abundance of mRNA was obtained by normalization to 18S levels.

Chromatin Immunoprecipitation Analysis

Chromatin immunoprecipitation (CHIP) analysis from mouse brains was performed using Magna Chip kit (Millipore) according to manufacturer's directions by using SIRT1 antibody (Upstate) and IgG. The primer sequences for proximal fragment are as the following: primer 1 forward, AGAAGCCGAAA GCCCTTCT; primer 1 reverse, GAGCGCTCTTTTCCCTGTG; primer 2 forward, AGGCCAATCCCTGCTC TC; primer 2 reverse, GACGGCACCCAATACACTC; primer 3 forward, TATCGCGGC TAAAATCATGG; primer 3 reverse, CTAC CCCGAAGCTGTCAAGA; primer 4 forward, GGCCTCGCGAGTGTATTG; primer 4 reverse, CTTCCCTGCCCTCGCT CT; upstream primer 1 forward, CAAACCCCAGGCTCTGTTTA; upstream primer 1 reverse, CAGGACCTCTGG AAG AGCAG; upstream primer 2 forward, CCAGCAACC ACATGGTGA; upstream primer 2 reverse, TTGATCTTTTGGGT TTGTTTCTC; upstream primer 3 forward, GAGAAACAAACCCAAAAGATCAA; and upstream primer 3 reverse, CCCTCTCCCAGGGTTCTCT.

Cells and Transfection

The plasmids pBABE-mSIRT1 and SIRT1$^{+/+}$ and SIRT1$^{-/-}$ MEFs have been described (Rockenstein et al., 2005). N2A cells were from ATCC. N2A cells stably overexpressing APPswe and PSEN1dE9 were kindly provided by Hyo-Jin Park and Seong Hun Kim (University of Florida). The plasmids expressing mSIRT1 and mSIRT1-HY were purchased from Addgene. Three SIRT1-shRNA plasmids and three ADAM10-shRNA plasmids were purchased from Open Biosystems. Transfections were performed by using Effectene transfection reagent (QIAGEN). ADAM10-shRNA sequences used were CCAGGAGAGTCTAAGAACTTA (shRNA 1), CAGCTCTA TATCCAGACAGAT (shRNA2), GAGTTATCAAATGGGACACAT (shRNA3), or siRNA (GCACAAAGU CUUAGAAUAUUU) for the 3′ UTR. ADAM10-ORF clone was purchased from Open Biosystems and siRNA against ADAM10 3′ UTR was purchased from Thermo Scientific. siRNA and ADAM10-ORF plasmid were cotransfected with DharmaFECT Duo transfection reagent from Thermo Scientific. Via PCR, silent mutations were introduced within the ADAM10 protein coding region (WT shRNA1 target: CCA GGA GAG TCT AAG AAC TTA; mutant shRNA1 target: CCC GGT GAA AGC AAA AAT CTC) to render the gene resistant to shRNA 1. Cells were treated with RA (Sigma) and LE 135 (Axon Medchem) of final concentration 1 μM and 5 μM, respectively as described (Li et al., 1999; Dollé et al., 1990).

Luciferase Assay

The plasmid expressing RARE-luciferase was purchased from Addgene. Cells were cotransfected with RARE-luciferase reporter and pRL-TK (*Renilla* luciferase; Promega), 24 hr later treated with RA and LE-135 for additional 48 hr. Luciferase activity was then measured by using the Dual-Luciferase Reporter Assay System (Promega). The final GL (firefly luciferase) activity was normalized to RL (*Renilla* luciferase) activity. The experiments were performed in triplicates and were repeated three times.

Statistical Analysis

The analysis was performed using Student's t test, and significant differences are demonstrated by single asterisk (*) indicating $p < 0.01$. Error bars in figures represent SEM.

SUPPLEMENTAL INFORMATION

Supplemental Information includes seven figures and can be found with this article online at doi:10.1016/j.cell.2010.06.020.

ACKNOWLEDGMENTS

We are grateful to Hyo-Jin Park and Seong Hun Kim for N2A APPswe/PSEN1dE9 cells. We thank Dennis Selkoe for helpful discussions. We also thank Takashi Nakagawa, Hung Chun Chang, and Petra Simic for comments on the manuscript. This work is supported by an American Parkinson Disease Association post-doctoral fellowship to G.D. and grants from the NIH and a gift from the Paul F. Glenn Foundation to L.G.

Received: January 19, 2010
Revised: March 12, 2010
Accepted: June 10, 2010
Published: July 22, 2010

REFERENCES

Araki, T., Sasaki, Y., and Milbrandt, J. (2004). Increased nuclear NAD biosynthesis and SIRT1 activation prevent axonal degeneration. Science *305*, 1010–1013.

Borchelt, D.R., Thinakaran, G., Eckman, C.B., Lee, M.K., Davenport, F., Ratovitsky, T., Prada, C.M., Kim, G., Seekins, S., Yager, D., et al. (1996). Familial Alzheimer's disease-linked Presenilin 1 variants elevate Aβ 1-42/1-40 ratio in vitro and in vivo. Neuron *17*, 1005–1013.

Bordone, L., Cohen, D., Robinson, A., Motta, M.C., van Veen, E., Czopik, A., Steele, A.D., Crowe, H., Marmor, S., Luo, J., et al. (2007). SIRT1 transgenic mice show phenotypes resembling calorie restriction. Aging Cell *6*, 759–767.

Bryan, K.J., Lee, H., Perry, G., Smith, M.A., and Casadesus, G. (2009). Transgenic mouse models of Alzheimer's disease: behavioral testing and considerations. In Methods of Behavior Analysis in Neuroscience, J.J. Buccafusco, ed. (Boca Raton, FL: CRC Press).

Cheng, H.L., Mostoslavsky, R., Saito, S., Manis, J.P., Gu, Y., Patel, P., Bronson, R., Appella, E., Alt, F.W., and Chua, K.F. (2003). Developmental defects and p53 hyperacetylation in Sir2 homolog (SIRT1)-deficient mice. Proc. Natl. Acad. Sci. USA *100*, 10794–10799.

Cao, D., Lu, H., Lewis, T.L., and Li, L. (2007). Intake of sucrose-sweetened water induces insulin resistance and exacerbates memory deficits and amyloidosis in a transgenic mouse model of Alzheimer Disease. J. Biol. Chem. *282*, 36275–36282.

Cohen, D.E., Supinski, A.M., Bonkowski, M.S., Donmez, G., and Guarente, L.P. (2009). Neuronal SIRT1 regulates endocrine and behavioral responses to calorie restriction. Genes Dev. *23*, 2812–2817.

Costa, R.M., Drew, J., and Silva, A.J. (2005). Notch to remember. Trends Neurosci. *28*, 429–435.

Corcoran, J.P.T., So, P.L., and Maden, M. (2004). Disruption of the retinoid signaling pathway causes a deposition of amyloid β in the adult rat brain. Eur. J. Neurosci. *20*, 896–902.

De Strooper, B. (2007). Loss-of-function presenilin mutations in Alzheimer disease. Talking Point on the role of presenilin mutations in Alzheimer disease. EMBO Rep. *8*, 141–146.

Dollé, P., Ruberte, E., Leroy, P., Morriss-Kay, G., and Chambon, P. (1990). Retinoic acid receptors and cellular retinoid binding proteins 1. A systemic study of their differential pattern of transcription during mouse organogenesis. Development *110*, 1133–1151.

Donmez, G., and Guarente, L. (2010). Aging and disease: connections to sirtuins. Aging Cell *9*, 285–290.

Fahrenholz, F., Prinzen, C., Postina, R., and Kojro, E. (2008). Up-regulation of the α-secretase pathway. In Advances in Alzheimer's and Parkinson's Disease, A. Fisher, ed. (New York: Springer), pp. 369–374.

Firestein, R., Blander, G., Michan, S., Oberdoerffer, P., Ogino, S., Campbell, J., Bhimavarapu, A., Luikenhuis, S., de Cabo, R., Fuchs, C., et al. (2008). The SIRT1 deacetylase suppresses intestinal tumorigenesis and colon cancer growth. PLoS ONE *3*, e2020.

Fukumoto, H., Rosene, D.L., Moss, M.B., Raju, S., Hyman, B.T., and Irizarry, M.C. (2004). β-secretase activity increases with aging in human, monkey and mouse brain. Am. J. Pathol. *164*, 719–725.

Goodman, A.B., and Pardee, A.B. (2003). Evidence for defective retinoid transport and function in late onset Alzheimer's disease. Proc. Natl. Acad. Sci. USA *100*, 2901–2905.

Goodman, A.B. (2006). Retinoid receptors, transporters, and metabolizers as therapeutic targets in late onset Alzheimer disease. J. Cell. Physiol. *209*, 598–603.

Guarente, L. (2009). Cell biology. Hypoxic hookup. Science *324*, 1289–1293.

Guarente, L. (2008). Mitochondria–a nexus for aging, calorie restriction and sirtuins? Cell *132*, 171–176.

Hardy, J., and Selkoe, D.J. (2002). The amyloid hypothesis of Alzheimer's disease: progress and problems on the road to therapeutics. Science *297*, 353–356.

Hartmann, D., Tournoy, J., Saftig, P., Annaert, W., and De Strooper, B. (2001). Implication of APP secretases in notch signaling. J. Mol. Neurosci. *17*, 171–181.

Jankowsky, J.L., Fadale, D.J., Anderson, J., Xu, G.M., Gonzales, V., Jenkins, N.A., Copeland, N.G., Lee, M.K., Younkin, L.H., Wagner, S.L., et al. (2004). Mutant presenilins specifically elevate the levels of the 42 residue β-amyloid peptide in vivo: evidence for augmentation of a 42-specific γ-secretase. Hum. Mol. Genet. *13*, 159–170.

Johansson, S., Jämsä, A., Vasänge, M., Winblad, B., Luthman, J., and Cowburn, R.F. (2006). Increased tau phosphorylation at the Ser396 epitope after amyloid beta-exposure in organotypic cultures. Neuroreport *17*, 907–911.

Kim, D., Nguyen, M.D., Dobbin, M.M., Fischer, A., Sananbenesi, F., Rodgers, J.T., Delalle, I., Baur, J.A., Sui, G., Armour, S.M., et al. (2007). SIRT1 deacetylase protects against neurodegeneration in models for Alzheimer's disease and amyotrophic lateral sclerosis. EMBO J. *26*, 3169–3179.

Kim, M., Suh, J., Romano, D., Truong, M.H., Mullin, K., Hooli, B., Norton, D., Tesco, G., Elliott, K., Wagner, S.L., et al. (2009). Potential late-onset Alzheimer's disease-associated mutations in the *ADAM10* gene attenuate α-secretase activity. Hum. Mol. Genet. *18*, 3987–3996.

Kojro, E., and Fahrenholz, F. (2005). The non-amyloidogenic pathway: structure and function of α-secretases. Subcell. Biochem. *38*, 105–127.

Kopan, R., and Ilagan, X.G. (2009). The canonical notch signaling pathway: unfolding the activation mechanism. Cell *137*, 216–233.

Lesné, S., Koh, M.T., Kotilinek, L., Kayed, R., Glabe, C.G., Yang, A., Gallagher, M., and Ashe, K.H. (2006). A specific amyloid-β protein assembly in the brain impairs memory. Nature *440*, 352–357.

Li, Y., Hashimoto, Y., Agadir, A., Kagechika, H., and Zhang, X. (1999). Identification of a novel class of retinoic acid receptor beta-selective retinoid antagonists and their inhibitory effects on AP-1 activity and retinoic acid-induced apoptosis in human breast cancer cells. J. Biol. Chem. *274*, 15360–15366.

Mangelsdorf, D.J., and Evans, R.M. (1995). The RXR heterodimers and orphan receptors. Cell *83*, 841–850.

Mangelsdorf, D.J., and Evans, R.M. (1992). Retinoid Receptors as Transcription Factors (Cold Spring Harbor, NY: Cold Spring Harbor Press).

Mattson, M.P. (1997). Cellular actions of beta-amyloid precursor protein and its soluble and fibrillogenic derivatives. Physiol. Rev. *77*, 1081–1132.

McBurney, M.W., Yang, X., Jardine, K., Hixon, M., Boekelheide, K., Webb, J.R., Lansdorp, P.M., and Lemieux, M. (2003). The mammalian Sir2a protein has a role in embryogenesis and gametogenesis. Mol. Cell. Biol. *23*, 38–54.

Milne, J.C., Lambert, P.D., Schenk, S., Carney, D.P., Smith, J.J., Gagne, D.J., Jin, L., Boss, O., Perni, R.B., Vu, C.B., et al. (2007). Small molecule activators of SIRT1 as therapeutics for the treatment of type 2 diabetes. Nature *450*, 712–716.

Panter, S.S., McSwigan, J.D., Sheppard, J.R., Emory, C.R., and Frey, W.H., 2nd. (1985). Glial fibrillary acidic protein and Alzheimer's disease. Neurochem. Res. *10*, 1567–1576.

Patel, N.V., Gordon, M.N., Connor, K.E., Good, R.A., Engelman, R.W., Mason, J., Morgan, D.G., Morgan, T.E., and Finch, C.E. (2005). Caloric restriction attenuates Aβ-deposition in Alzheimer transgenic models. Neurobiol. Aging *26*, 995–1000.

Postina, R., Schroeder, A., Dewachter, I., Bohl, J., Schmitt, U., Kojro, E., Prinzen, C., Endres, K., Hiemke, C., Blessing, M., et al. (2004). A disintegrin-metalloproteinase prevents amyloid plaque formation and hippocampal defects in an Alzheimer disease mouse model. J. Clin. Invest. *113*, 1384–1387.

Pozniak, C.D., Barnabé-Heider, F., Rymar, V.V., Lee, A.F., Sadikot, A.F., and Miller, F.D. (2002). p73 is required for survival and maintenance of CNS neurons. J. Neurosci. *22*, 9800–9809.

Prinzen, C., Müller, U., Endres, K., Fahrenholz, F., and Postina, R. (2005). Genomic structure and functional characterization of the human ADAM10 promoter. FASEB J. *19*, 1522–1524.

Qin, W., Yang, T., Ho, L., Zhao, Z., Wang, J., Chen, L., Zhao, W., Thiyagarajan, M., MacGrogan, D., Rodgers, J.T., et al. (2006). Neuronal SIRT1 activation as a novel mechanism underlying prevention of Alzheimer Disease amyloid neuropathology by calorie restriction. J. Biol. Chem. *281*, 21745–21754.

Reiserer, R.S., Harrison, F.E., Syverud, D.C., and McDonald, M.P. (2007). Impaired spatial learning in the APPswe, PSEN1dE9 bigenic mouse model of Alzheimer's disease. Genes Brain Behav. *6*, 54–65.

Rockenstein, E., Mante, M., Alford, M., Adame, A., Crews, L., Hashimoto, M., Esposito, L., Mucke, L., and Masliah, E. (2005). High beta-secretase activity elicits neurodegeneration in transgenic mice despite reductions in amyloid-beta levels: implications for the treatment of Alzheimer disease. J. Biol. Chem. *280*, 32957–32967.

Saftig, P., and Hartmann, D. (2005). ADAM10. In The ADAM Family of Proteases, N.M. Hooper and U. Lendeckel, eds. (Dordrecht, The Netherlands: Springer), pp. 85–121.

Selkoe, D.J. (1997). Alzheimer's disease: genotypes, phenotypes and treatments. Science *275*, 630–631.

Sinclair, D.A. (2005). Toward a unified theory of caloric restriction and longevity regulation. Mech. Ageing Dev. *126*, 987–1002.

Tanzi, R.E., and Bertram, L. (2005). Twenty years of the Alzheimer's disease amyloid hypothesis: a genetic perspective. Cell *120*, 545–555.

Tippmann, F., Hundt, J., Schneider, A., Endres, K., and Fahrenholz, F. (2009). Up-regulation of the α-secretase ADAM10 by retinoic acid receptors and acitretin. FASEB J. *23*, 1643–1654.

van Tetering, G., van Diest, P., Verlaan, I., van der Wall, E., Kopan, R., and Vooijs, M. (2009). The metalloprotease ADAM10 is required for Notch1 S2 cleavage. J. Biol. Chem. *284*, 31018–31027.

Vieira, S.I., Rebelo, S., Domingues, S.C., da Cruz e Silva, E.F., and da Cruz e Silva, O.A. (2009). S655 phosphorylation enhances APP secretory traffic. Mol. Cell. Biochem. *328*, 145–154.

Yoon, K., and Gaiano, N. (2005). Notch signaling in the mammalian central nervous system: insights from mouse mutants. Nat. Neurosci. *8*, 709–715.